Numerical Methods of Estimating Bounds on the Non-linear Saturation of Barotropic Instability

By Keiichi Ishioka
Department of Mathematical Sciences, University of Tokyo, Tokyo 153, Japan

and

Shigeo Yoden
Department of Geophysics, Kyoto University, Kyoto 606-01, Japan

(Manuscript received 19 December 1994, in revised form 22 November 1995)

Journal of the Meteorological Society of Japan
Vol. 74, No.2
Meteorological Society of Japan

Journal of the Meteorological Society of Japan, Vol. 74, No. 2, pp. 167–174, 1996

Numerical Methods of Estimating Bounds on the Non-linear Saturation of Barotropic Instability

By Keiichi Ishioka

Department of Mathematical Sciences, University of Tokyo, Tokyo 153, Japan

and

Shigeo Yoden

Department of Geophysics, Kyoto University, Kyoto 606-01, Japan

(Manuscript received 19 December 1994, in revised form 22 November 1995)

Abstract

Two numerical methods are presented for calculating rigorous upper bounds on the finite-amplitude growth of barotropic instabilities to zonal jets on a rotating sphere.

One of the methods is based on Shepherd (1988)'s analytic method, which uses the conservation law of domain-averaged pseudomomentum density. A variational minimization problem is solved numerically with a quasi-Newton method after discretization. The other is the authors' original method to solve a minimization problem under the constraints of the conservation laws of all Casimir invariants and total absolute angular momentum. The convex simplex method, which has been used in operations research, is applied to solve a quadratic programming problem.

The two methods are applied to estimate the upper bounds for several profiles of the initial unstable jet and the bounds are compared with the results of non-linear time integrations from the unstable jet with a high-resolution model (Ishioka and Yoden, 1994). The two bounds are found to be almost completely identical to each other. Evidence from high-resolution numerical experiments is that the bounds overestimate the actual wave-enstrophy achieved in numerical experiments by a factor of 1.2 to 2.3.

1. Introduction

Barotropic (or shear) instability of zonal jets is an interesting subject not only of theoretical fluid dynamics but also of dynamic meteorology because several atmospheric phenomena are thought to be caused by the instability such as the traveling waves in the southern hemisphere upper stratosphere (see, *e.g.*, Hartmann 1983). When a zonal jet is barotropically unstable, disturbances grow exponentially to have a finite amplitude. Ishioka and Yoden (1994, hereafter referred to as IY94) numerically investigated the non-linear evolution of a polar night jet of which linear stability was originally investigated by Hartmann (1983). In that study a question arose naturally: "How large can the disturbances grow depending on the initial state?"

Shepherd (1988) gave a general solution to this kind of question. He presented a novel method to obtain rigorous, full-non-linear upper bounds of the growth of the disturbances, and applied the method to various zonal flow profiles to calculate the upper bounds analytically. However, he did not bother himself to get tighter bounds by numerical means, since his interest lay in the theoretical side of the problem. Thus, in this study, we explore numerical methods to compute tighter bounds. A new method is proposed in addition to an application of Shepherd's method. The obtained bounds for several unstable polar night jets are compared with the result of non-linear time integrations of IY94 and that of additional experiments newly conducted for this paper.

The governing equation and theoretical basis of bounds are described in Section 2. The numerical procedures are presented in Section 3, and the jet profiles and non-linear time integrations we analyze are described in Section 4. Results are given in Section 5, discussion is in Section 6, and conclusions are in Section 7.

2. Basic equations and theoretical basis of bounds

The system under consideration is non-divergent two-dimensional flow on the earth, which flow is governed by the conservation law of the absolute vorticity $q(\lambda,\mu,t)\equiv\zeta+2\Omega\mu$ following the fluid motion:

$$\frac{Dq}{Dt}\equiv\frac{\partial q}{\partial t}+\frac{1}{a^2}\left(\frac{\partial\psi}{\partial\lambda}\frac{\partial q}{\partial\mu}-\frac{\partial\psi}{\partial\mu}\frac{\partial q}{\partial\lambda}\right)=0, \tag{1}$$

where $\zeta(\lambda,\mu,t)$ is vorticity ($\zeta\equiv\nabla^2\psi$), $\psi(\lambda,\mu,t)$ is the streamfunction, λ is longitude, $\mu\equiv\sin\phi$, ϕ is latitude, t is time, a is the radius of the earth ($=6.37\times10^6$ m), Ω is the angular speed of rotation of the earth ($=7.29\times10^{-5}$/s), and ∇^2 is the horizontal Laplacian:

$$\nabla^2\equiv\frac{1}{a^2}\frac{1}{1-\mu^2}\frac{\partial^2}{\partial\lambda^2}+\frac{1}{a^2}\frac{\partial}{\partial\mu}\left\{(1-\mu^2)\frac{\partial}{\partial\mu}\right\}. \tag{2}$$

In this system, the following three kinds of quantities are conserved: "Casimir invariant" $C_f\equiv[\overline{f(q)}]$, total absolute angular momentum $D\equiv[\mu\overline{q}]$, and total kinetic energy $E\equiv[-\frac{1}{2}\overline{\psi\zeta}]$, where $f(q)$ is an arbitrary function of q, and $\overline{(\ )}$ and $[(\ )]$ represent zonal mean and latitudinal mean, respectively. That is,

$$\overline{(\ )}\equiv\frac{1}{2\pi}\int_0^{2\pi}(\ )d\lambda,\quad[(\ )]\equiv\frac{1}{2}\int_{-1}^{1}(\ )d\mu. \tag{3}$$

Now we consider the upper bounds of the growth of the disturbances. From the conservation law of C_f, total absolute enstrophy $F\equiv[\frac{1}{2}\overline{q^2}]$ is also an invariant. The total enstrophy F is divided into zonal enstrophy F_z and wave-enstrophy F_w:

$$F=F_z+F_w, \tag{4}$$

$$F_z\equiv\left[\frac{1}{2}\overline{q}^2\right],\quad F_w\equiv\left[\frac{1}{2}\overline{q'^2}\right], \tag{5}$$

where $q'\equiv q-\overline{q}$. In the following subsections, the upper bounds to F_w are considered for the evolution from an initial q distribution which consists of an unstable zonal state $\overline{q}_0(\mu)$ and infinitesimal disturbances.

a. An obvious bound

Considering only the conservation law of the angular momentum D, a minimum of F_z which could be attainable is obtained by a simple calculation as given in the Appendix:

$$(F_z)_{\min}=\frac{3}{2}D^2=\frac{3}{2}[\mu\overline{q}_0(\mu)]^2. \tag{6}$$

Then an obvious maximum bound F_0 to the wave-enstrophy F_w is obtained from (4),

$$F_0=(F_w)_{\max}=F-(F_z)_{\min}=F-\frac{3}{2}D^2$$
$$=\left[\frac{1}{2}\overline{q}_0(\mu)^2\right]-\frac{3}{2}[\mu\overline{q}_0(\mu)]^2. \tag{7}$$

Here the conservation law of a single Casimir F as well as that of the angular momentum D was used to get the obvious bound F_0.

b. Shepherd's bounds

If we define the pseudomomentum density as follows:

$$A(Q,q)\equiv-\int_Q^q\{Y(\eta)-Y(Q)\}d\eta, \tag{8}$$

then $[\overline{A(Q,q)}]$ becomes an invariant as described in Shepherd (1987). Here, $Q(\mu)$ is an arbitrary monotonic function of μ and $Y(\eta)$ is its inverse function. Note that the present notation of q is different from Shepherd's definition; the present q is identical to his $Q+q$. When non-linear stability is considered, Q is a 'basic state' and $q-Q$ is a finite-amplitude disturbance. This conservation law is easily deduced from the conservation laws of a single Casimir C_f and D (see McIntyre and Shepherd, 1987). For this invariant, the following inequalities hold:

$$|Y'|_{\min}\left[\frac{1}{2}\overline{(q-Q)^2}\right]\le|[\overline{A(Q,q)}]|$$
$$=|[A(Q,\overline{q}_0)]|\le|Y'|_{\max}\left[\frac{1}{2}(\overline{q}_0-Q)^2\right]. \tag{9}$$

Utilizing (9) and the following inequality for F_w:

$$F_w=\left[\frac{1}{2}\overline{q'^2}\right]\le\left[\frac{1}{2}\overline{q'^2}\right]+\left[\frac{1}{2}(\overline{q}-Q)^2\right]$$
$$=\left[\frac{1}{2}\overline{(q-Q)^2}\right], \tag{10}$$

the bounding inequalities for F_w are obtained:

$$F_w\le\frac{1}{|Y'|_{\min}}|[A(Q,\overline{q}_0)]|$$
$$\le\frac{|Y'|_{\max}}{|Y'|_{\min}}\left[\frac{1}{2}(\overline{q}_0-Q)^2\right]. \tag{11}$$

Now two bounds F_1 and F_2 for F_w are obtained:

$$F_1\equiv\min\left(\frac{|Y'|_{\max}}{|Y'|_{\min}}\left[\frac{1}{2}(\overline{q}_0-Q)^2\right]\right), \tag{12}$$

$$F_2\equiv\min\left(\frac{1}{|Y'|_{\min}}|[A(Q,\overline{q}_0)]|\right), \tag{13}$$

where min ( ) is taken over arbitrary choices of monotonic function $Q(\mu)$. Although Shepherd (1987) had derived the inequality (11), Shepherd (1988) utilized only the bound F_1. Thus we call the bound F_1 "original Shepherd's bound", and the bound F_2 "revised Shepherd's bound". It is obvious that F_2 is tighter than F_1.

c. A direct bound

In the Subsections 2.*a* and 2.*b*, we have used only the conservation of angular momentum and a single Casimir as a constraint. However, if the conservation of all Casimir invariants is also included as a constraint, $(F_z)_{\min}$ must be larger than the estimate of (6). That is, if we can examine all $q(\lambda,\mu)$ distributions which are rearrangements of the initial distribution of $\overline{q}_0(\mu)$ under the constraint of the

conservation of D, a tighter bound will be obtained as:

$$F_3 \equiv F - \min(F_z), \tag{14}$$

where min ( ) is taken over all the possible distributions of q. Note that any C_f is conserved in the rearrangements of q distribution. It is obvious that the following inequalities hold for the bounds F_0, F_1, F_2, and F_3:

$$F_w \leq F_3 \leq F_2 \leq F_1 \leq F_0. \tag{15}$$

3. Numerical procedures

a. An obvious bound

To compute the obvious bound F_0, the values of the invariants F and D must be calculated for a given initial profile $\overline{q}_0(\mu)$. We compute the integration for μ which appears in Eq. (7) using the Gauss-Legendre quadrature formula (see Press, *et al.*, 1992, hereafter referred to as *Numerical Recipes*). The number of the Gaussian latitudes we have used is up to 100, which is sufficient for the $\overline{q}_0(\mu)$ profiles given in the next section.

b. Shepherd's bounds

To calculate Shepherd's bounds F_1 and F_2, the variational minimization problems (12) and (13) must be solved. For computation, we discretize the monotonic function $Q(\mu)$ into N straight segments as

$$Q(\mu) = \frac{Q_i - Q_{i-1}}{Y_i - Y_{i-1}}(\mu - Y_{i-1}) + Q_{i-1} \quad (Y_{i-1} \leq \mu \leq Y_i)\ (i = 1, 2, \cdots, N), \tag{16}$$

where $Q_i = Q|_{\mu = Y_i}$. Since $Q(\mu)$ must be monotonic (we deal with a monotonically increasing function $Q(\mu)$; it is easy to apply the following discussion to monotonically decreasing function), we introduce parameters α_i and β_i $(i = 1, 2, \cdots, N)$ and represent the nodes (Q_i, Y_i) by them as follows:

$$\frac{Q_{i+1} - Q_i}{Q_i - Q_{i-1}} = e^{\alpha_i}, \quad \frac{Y_{i+1} - Y_i}{Y_i - Y_{i-1}} = e^{\beta_i} \quad (i = 1, 2, \cdots, N - 1), \tag{17}$$

$$(Q_0, Y_0) = \begin{cases} (\, q_{\min}, & -1 - \alpha_N\,) & (\alpha_N \geq 0) \\ (\, q_{\min} + \alpha_N, & -1\,) & (\alpha_N < 0), \end{cases}$$
$$(Q_N, Y_N) = \begin{cases} (\, q_{\max}, & 1 + \beta_N\,) & (\beta_N \geq 0) \\ (\, q_{\max} - \beta_N, & 1\,) & (\beta_N < 0), \end{cases} \tag{18}$$

where $q_{\min}$ and $q_{\max}$ are the minimum and maximum of $\overline{q}_0(\mu)$, respectively. Equation (18) comes from the necessity that the domain of $Q(\mu)$ and that of its inverse $Y(\eta)$ must include the domain $[-1, 1]$ and $[q_{\min}, q_{\max}]$, respectively. That is, the following inequalities:

$$Q_0 \leq q_{\min},\ q_{\max} \leq Q_N,\ Y_0 \leq -1,\ 1 \leq Y_N, \tag{19}$$

must hold. The ends (Q_0, Y_0) and (Q_N, Y_N) can move, satisfying the above constraints by changing the values of α_N and β_N. Solving the Eq. (17) simultaneously for given parameters (α_i, β_i) $(i = 1, 2, \cdots, N-1)$ with the ends (Q_0, Y_0) and (Q_N, Y_N) determined by Eq. (18), the nodes (Q_i, Y_i) $(i = 1, 2, \cdots, N-1)$ are determined to satisfy the following inequalities:

$$Q_0 < Q_1 < \cdots < Q_N,\ Y_0 < Y_1 < \cdots < Y_N. \tag{20}$$

Then the variational problems (12) and (13) are translated into an unrestricted optimization problem for $2N$ variables (α_i, β_i) by representing the nodes (Q_i, Y_i) by them. Computing the integration for μ in (12) or (13) with the Gauss-Legendre quadrature formula, the optimization problem can be solved by various numerical methods. We have employed a library subroutine for the minimization based on a quasi-Newton method (see *Numerical Recipes*) for its quick convergence. The number of segments (N) we have used is from 10 to 50. The reason is that larger N does not necessarily give tighter bounds because the numerical optimization may converge to a spurious local minimum when N is too large.

c. A direct bound

Employing the Gauss-Legendre quadrature formula as a discretizing method again, we divide the whole sphere into M zonal bands: The area of each band is set to be $2\pi a^2 \cdot w_j$ $(j = 1, 2, \cdots, M)$, where w_j is a Gaussian weight. Namely, the width of each band is w_j in μ-coordinates. Now we consider movement of an air parcel between the zonal bands during the non-linear saturation process of barotropic instability. Here, note that we do not assume a zonally symmetric rearrangement. If we write the area of air parcel that has moved from the initial i-th band to the final j-th band as $2\pi a^2 \cdot r_{ij}$ $(i = 1, 2, \cdots, M,\ j = 1, 2, \cdots, M)$, r_{ij} is subject to the following constraints:

$$\sum_{i=1}^{M} r_{ij} = w_j \ (j = 1, 2, \cdots, M), \tag{21}$$

$$\sum_{j=1}^{M} r_{ij} = w_i \ (i = 1, 2, \cdots, M), \tag{22}$$

$$r_{ij} \geq 0 \ (i = 1, 2, \cdots, M,\ j = 1, 2, \cdots, M). \tag{23}$$

Here, the constraints (21) and (22) mean the conservation of the area of parcels (or mass) and (23) is required because the area can not be negative. The same type of constraints appear in the *transportation problem* in operations research. Note that one of the equations in (21) and (22) is automatically satisfied if the other $2M - 1$ equations are satisfied; that is, the dimension of the constraint is $2M - 1$.

Assuming the material conservation of q and using r_{ij}, the zonal mean absolute vorticity in the final state $\overline{q}_j$ is represented as follows:

$$\overline{q}_j = \frac{1}{w_j}\sum_{i=1}^{M} q_i r_{ij} \ (j = 1, 2, \cdots, M), \tag{24}$$

where $q_i = \overline{q}_0(\mu_i)$ $(i = 1, 2, \cdots, M)$. Then the conservation law of the angular momentum D is represented as:

$$\frac{1}{2}\sum_{j=1}^{M} w_j \mu_j \overline{q}_j = D \left(= \frac{1}{2}\sum_{i=1}^{M} w_i \mu_i q_i\right), \tag{25}$$

and the zonal enstrophy is written as:

$$F_z = \frac{1}{2}\sum_{j=1}^{M} w_j \frac{1}{2}(\overline{q}_j)^2. \tag{26}$$

Now the procedure to get the direct bound is completed; "minimize F_z defined as (26) under the constraints (21), (22), (23), and (25), then the direct bound (F_3) is obtained by (14)". This is a *quadratic programming problem* which also appears in operations research. We have solved this problem numerically employing the *Convex Simplex Method* (see, *e.g.*, Luenberger, 1973) for its robustness and simplicity. The number of zonal bands M we used was up to 100, which is sufficient for the $\overline{q}_0(\mu)$ profiles given in the next section.

4. Jet profiles and non-linear time integrations

Two types of jet profiles introduced by Hartmann (1983), which are idealization of polar night jets in the stratosphere, are analyzed to compare the four bounds $F_0 - F_3$ with the result of non-linear time integrations we have done in our previous work (IY94). The two types of the profiles are defined as follows:

$$\text{tanh-type jet: } \overline{u}_0(\phi) = U\cos\phi \cdot \frac{1}{2}\left(1 + \tanh\frac{\phi - \phi_0}{B}\right), \tag{27}$$

$$\text{sech-type jet: } \overline{u}_0(\phi) = U\cos\phi \cdot \operatorname{sech}\frac{2(\phi - \phi_0)}{B}, \tag{28}$$

where U is a measure of the intensity of the jet, B is its width, and ϕ_0 is its position. The tanh-type jet has a negative latitudinal gradient of zonal mean absolute vorticity on the equatorward flank of the jet axis, while the sech-type jet has that mainly on the poleward flank of the jet axis. Then the initial profile of zonal mean absolute vorticity $\overline{q}_0(\mu)$ is given as:

$$\overline{q}_0(\mu) \equiv -\frac{1}{a}\frac{d}{d\mu}\left(\sqrt{1-\mu^2}\overline{u}_0\right) + 2\Omega\mu. \tag{29}$$

In the non-linear time integrations in IY94, an artificial viscosity term was introduced on the right-hand side of Eq. (1) to smooth numerical behavior:

$$\frac{Dq}{Dt} = \nu\left(\nabla^2 + \frac{2}{a^2}\right)q, \tag{30}$$

where the conservation law of angular momentum requires the second term $2/a^2$ in the parentheses. Throughout IY94, the viscosity coefficient ν was fixed at a small constant which gives the dissipation time-scale of 1 day at the largest total wavenumber ($n = 170$) in the model.

The viscosity term introduced above is a normal one, with which the basic equation becomes the two-dimensional Navier-Stokes equation. However, direct comparison between the bounds and the result of the numerical experiments becomes rather difficult, since the bounding theories described in the previous section are for inviscid fluid. Therefore, we have conducted additional experiments to emulate inviscid fluid better with a hyper-viscosity term instead of the normal viscosity term. The equation we have used is:

$$\frac{Dq}{Dt} = -\nu_h\left(\nabla^2 + \frac{2}{a^2}\right)^{10} q, \tag{31}$$

where the hyper-viscosity coefficient ν_h is set to give the dissipation time-scale of 0.01 days at the largest total wavenumber.

The non-linear Eqs. (30) and (31) are integrated numerically from an initial state $q = \overline{q}_0(\mu) + q_d(\lambda, \mu)$, where $\overline{q}_0$ is the intial zonal profile defined above and $q_d(\lambda, \mu)$ is an initial disturbance defined as;

$$q_d(\lambda, \mu) \equiv \alpha\left(e^{\beta(\cos\theta - 1)} - \frac{1 - e^{-2\beta}}{2\beta}\right), \tag{32}$$

$$\cos\theta \equiv \mu\mu_d + \sqrt{(1-\mu^2)(1-\mu_d^2)}\cos(\lambda - \lambda_d). \tag{33}$$

Here α and β are measures of the intensity and horizontal extent of the disturbance, respectively. The center of the disturbance is given by (λ_d, μ_d) and θ is angular distance from the center. The initial disturbance is a Gaussian-like smooth function on a sphere, which is easily confirmed because $q_d \to \alpha(e^{-\beta\theta^2/2} - \frac{1-e^{-2\beta}}{2\beta})$ as $\theta \to 0$. The second term in the parentheses in Eq. (32) is required for $[\overline{q_d}]$ to be 0. We have chosen the initial disturbance with small α and large β, which gives nearly white spectra in the wavenumber space, to investigate behavior of waves raised by the instability of the basic zonal flow itself.

While the disturbance parameters were fixed as $\alpha = 0.01\Omega, \beta = 100$, and $(\lambda_d, \mu_d) = (0°, \sin 45°)$ in IY94, in the additional experiments three values of $\mu_d = \sin 30°, \sin 45°$, and $\sin 60°$ are used to examine the dependence of the results on the initial disturbance.

The advection term is computed using a spectral transform method with a triangular truncation of T170. The fourth order Runge-Kutta method is used for time integrations with an increment of

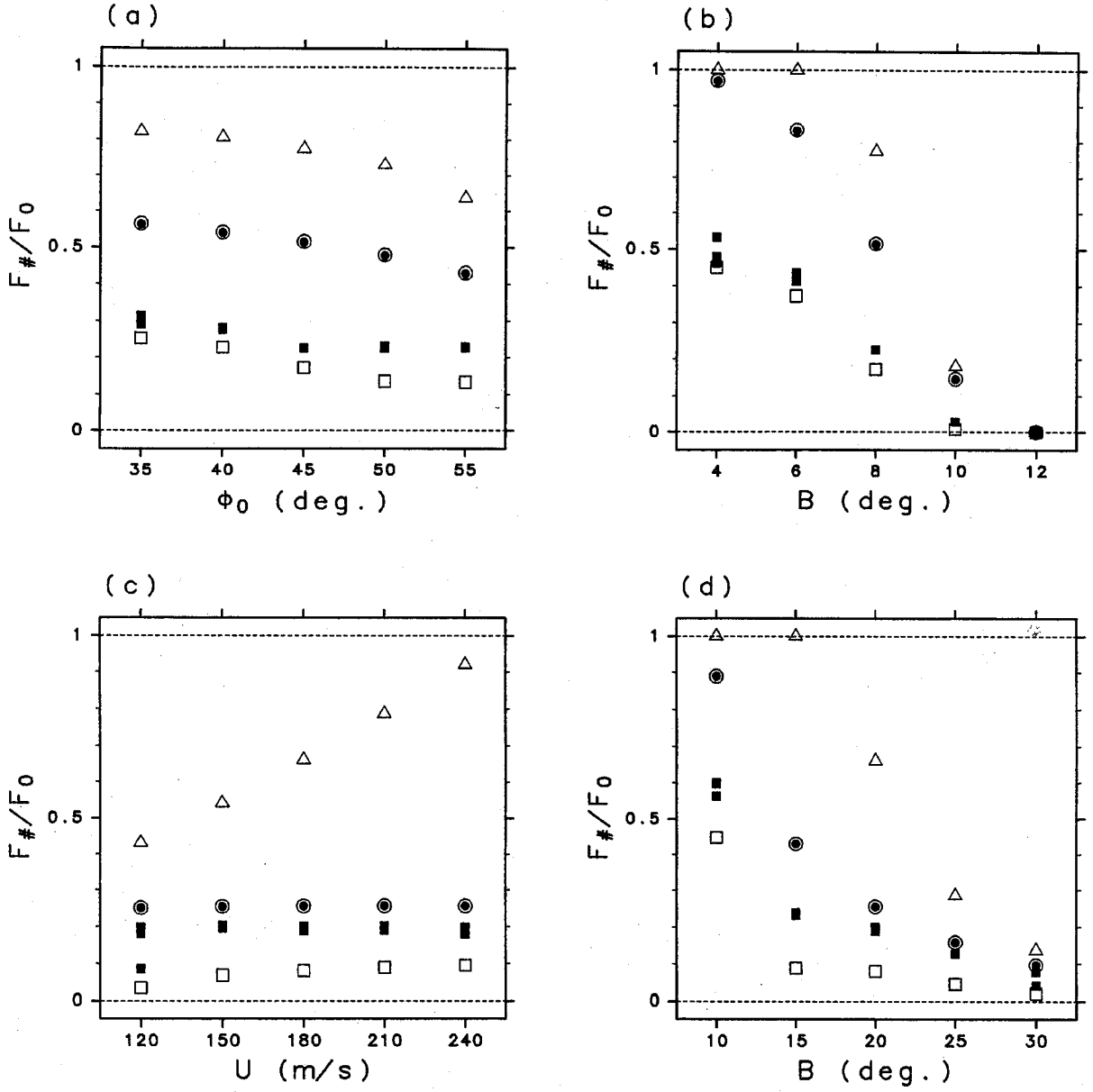

Fig. 1. Comparison among the bounds F_1 (triangles), F_2 (circles), and F_3 (bullets) and the maximum wave-enstrophy F_4 (open squares for normal viscosity and closed squares for hyper-viscosity). Each value is normalized by the obvious bound F_0. (a): tanh-type jet with $U = 180$ m/s, $B = 8°$, and ϕ_0 varying from 35° to 55°, (b): tanh-type jet with $U = 180$ m/s, $\phi_0 = 45°$, and B varying from 4° to 12°, (c): sech-type jet with $\phi_0 = 60°$, $B = 20°$, and U varying from 120 m/s to 240 m/s, and (d): sech-type jet with $U = 180$ m/s, $\phi_0 = 60°$, and B varying from 10° to 30°. See the text for the meaning of $F_1 - F_4$.

0.01 days. Wave-enstrophy F_w is computed in every time-step during the integration period (100 days) to determine $(F_w)_{\max}$. Hereafter we refer to the maximum as F_4.

5. Results

a. Comparison among the bounds

Figure 1 compares the bounds F_1, F_2, and F_3, with the maximum wave-enstrophy F_4 obtained in numerical time integrations. Each value is normalized by the obvious bound F_0. (a) and (b) are for the tanh-type jet; (a): $U = 180$ m/s, $B = 8°$, and ϕ_0 varying over the values 35°, 40°, 45°, 50°, and 55°, (b): $U = 180$ m/s, $\phi_0 = 45°$, and B varying over the values 4°, 6°, 8°, 10°, and 12°. (c) and (d) are for the sech-type jet; (c): $\phi_0 = 60°$, $B = 20°$, and U varying over the values 120 m/s, 150 m/s, 180 m/s, 210 m/s, and 240 m/s, (d): $U = 180$ m/s, $\phi_0 = 60°$, and B varying over the values 10°, 15°, 20°, 25°, and 30°.

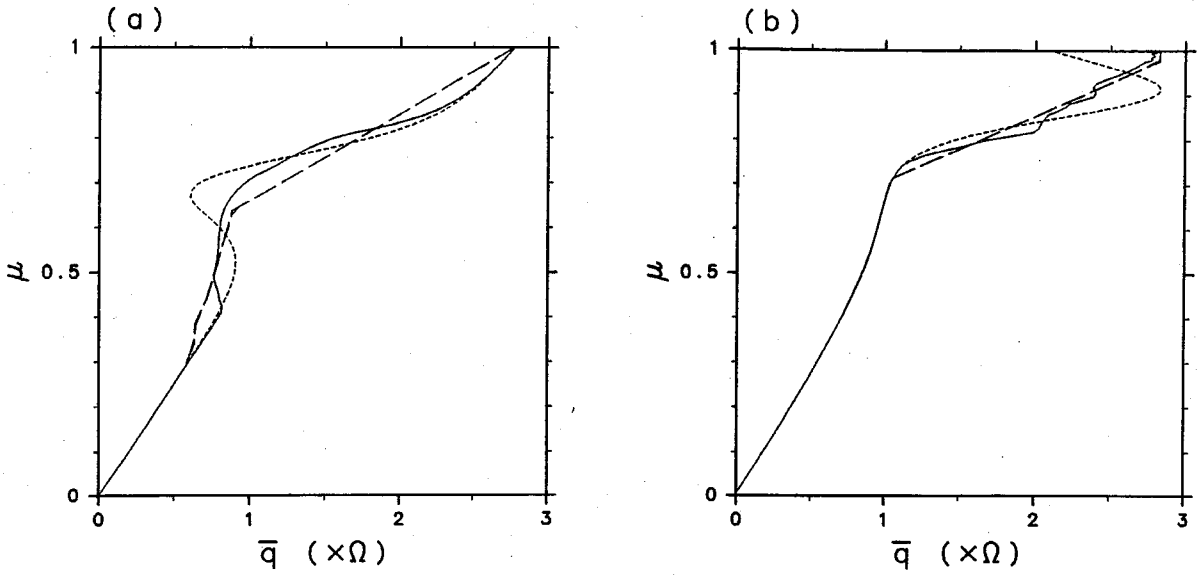

Fig. 2. Comparison among zonal mean profiles of absolute vorticity. The dotted line is the initial profile $\overline{q}_0(\mu)$, the broken line is $Q(\mu)$ for the revised Shepherd's bound and the $\overline{q}_j$ profile that gives the direct bound, and the solid line is the profile corresponding to the maximum wave-enstrophy in non-linear time integrations. (a): tanh-type jet with $U = 180$ m/s, $\phi_0 = 45°$, and $B = 8°$, and (b): sech-type jet with $U = 180$ m/s, $\phi_0 = 60°$, and $B = 20°$.

To begin with, comparing the original Shepherd's bound F_1 (triangles) with revised Shepherd's bound F_2 (circles), the revised bound is much tighter than the original bound for all parameter ranges. In particular, the difference between these two bounds is remarkable in (c); the original bound F_1 gets larger with U, while the revised bound F_2 is nearly constant with U. In (b) and (d), the original bound becomes equal to the obvious bound when the jet is narrow (*i.e.* $B = 4°$ and $6°$ in (b) and $B = 10°$ and $15°$ in (d)). On the other hand, the revised bound gives a tighter bound, even in these cases.

Secondly, let us compare the revised bound F_2 with our direct bound F_3 (bullets). Surprisingly, the two bounds are almost completely identical within the relative difference of 0.5 % for all parameter ranges shown in Fig. 1. This difference seems due to the finite values N and M in the numerical discretizations.

Finally, let us compare these bounds with the result of non-linear time integrations. The maximum wave-enstrophy F_4 in the experiments of normal viscosity (open squares) is smaller than that in the hyper-viscosity experiments (closed squares) in particular for the sech-type jet, (c) and (d). This is because the growth rate of unstable modes for the sech-type jets is so small that the effect of viscosity cannot be neglected. Therefore, hereafter we refer to $(F_4)_{\max}$ as the largest of the three of the hyper-viscosity results. In all parameter ranges in Fig. 1, revised Shepherd's bound and the direct bound give good estimates of the dependence of $(F_4)_{\max}$ on the external parameters which determine the initial jet profiles, although these bounds exceed $(F_4)_{\max}$ by a factor of 1.2 to 2.3 except for the cases of weak instability: the tanh-type jet with $B = 10°$ and $12°$ in (b). In particular, the maximum wave-enstrophy is very close to the bound in (c), where $F_3/(F_4)_{\max} \sim 1.3$ for all five values of U.

b. Meridional profiles of zonal mean absolute vorticity

Figure 2 shows the meridional profiles of zonal mean absolute vorticity for the tanh-type jet with $U = 180$ m/s, $\phi_0 = 45°$, and $B = 8°$ (a), and for the sech-type jet with $U = 180$ m/s, $\phi_0 = 60°$, and $B = 20°$ (b). The initial profile $\overline{q}_0(\mu)$ has negative $d\overline{q}_0(\mu)/d\mu$, as shown by a dotted line. The solid line is the $\overline{q}(\mu)$ profile that corresponds to $(F_4)_{\max}$, which is achieved by the initial disturbance with $\mu_d = \sin 60°$ for the tanh-type jet and $\mu_d = \sin 30°$ for the sech-type jet. Note that the initial negative $d\overline{q}_0(\mu)/d\mu$ disappears in almost all the latitudes. The $Q(\mu)$ profile for the revised Shepherd's bound (dashed line) is almost completely identical to the $\overline{q}_j$ profile that gives the direct bound (it looks like the same dashed line). This is also an interesting result because there is no *a priori* reason why they should agree. These two profiles have a positive gradient in all the latitudes and give an estimate of $\overline{q}(\mu)$. Corresponding to the closeness between the maximum wave-enstrophy and the bound in Fig. 1, the realized profile is very similar to the $\overline{q}_j$ profile for the sech-type jet (b) while it is not the case for the tanh-

type jet (a). A straight segment appears in $Q(\mu)$ (or $\overline{q}_j$) profiles in both cases and its latitudinal gradient has a maximum value there. The existence of such a straight segment is predicted mathematically by Haynes for the Shepherd's bound (see Appendix C in Shepherd (1988)).

6. Discussion

The most interesting result in the previous section is the identity between the revised Shepherd's bound and our direct bound. Such an identity is seen not only for the profiles analyzed in this paper but also for other profiles such as $\overline{q}_0(\mu) = a_3 P_3(\mu) + 2\Omega\mu$, which is one of the simplest profiles that can be unstable. Here, $P_3(\mu)$ is a third-order Legendre polynomial (see the Appendix for its definition) and a_3 is its coefficient. This implies that the revised Shepherd's bound gives the tightest bound under the constraints of the conservation of all Casimir invariants and total angular momentum. However, the proof of the above conjecture is a problem to be solved in further investigations. If the above conjecture always holds, the revised Shepherd's bound is more economical in computation of the bound because the number of variables in the computation of the Shepherd's bound ($2N$) is much smaller than that of the direct bound (M^2) when $N \sim M \gg 1$. Furthermore, our choice of representation in the computation of the Shepherd's bound is contributing to the economy because the $Q(\mu)$ profile can be represented well by small number of nodes (Q_i, Y_i) owing to the nature that the $Q(\mu)$ profile which gives the bound should have a straight segment, as shown in Fig. 2.

Another problem we have to discuss here is the difference between the revised Shepherd's bound (or our direct bound) and the maximum wave-enstrophy in the non-linear time integrations. There are four possible reasons for the difference: (1) The bound is still loose because the energy conservation is not included as a constraint. (2) The artificial hyper-viscosity term in Eq. (31) for the non-linear time integrations may prevent the wave-enstrophy from having a true maximum. (3) The wave-enstrophy need not attain the maximum value estimated in the bounding theories. (4) The prescribed initial disturbance may not be optimal for disturbances to grow. By the aid of the additional experiments we can rule out the possibility (2) because the decay of the total enstrophy is too small to fill the gap between the bound and the maximum wave-enstrophy in the experiments with the hyper-viscosity. For example, the decay is 0.19 % of F_0 while $F_3 - (F_4)_{\max}$ is 29 % of F_0 for the tanh-type jet with $U = 180$ m/s, $\phi_0 = 45°$, and $B = 8°$. Next, let us consider the possibility (4). Since it is impossible to examine "all" kinds of initial disturbances, we cannot remove the possibility. However, the dependence on the initial disturbance in the three experiments seems so small that it is not imaginable that there would be a special kind of initial disturbance which can take the disturbance up to the bound. Now two possibilities, (1) and (3), are left. To make sure which is the most important reason, a new method for estimating bounds with the constraint of the energy conservation must be developed. Energy conservation may hold a key to explain why the bound is very tight for the sech-type jets while it is not for the tanh-type jets. Furthermore, the bound on energy is more suitable than that on enstrophy, since a certain amount of the decay of the total enstrophy is inevitable for the experiment to be valid, whatever numerical method is used. This energy bound will be obtained if we can develop the method to include energy conservation, which is also a difficult problem we would like to try to solve in our future work.

7. Conclusions

Numerical methods to compute Shepherd (1988)'s rigorous upper bounds on the finite-amplitude growth of barotropic instabilities to zonal jets were explored and a novel method was presented to obtain a "direct" bound which includes the conservation law of all Casimir invariants and total absolute angular momentum as the constraints. The convex simplex method was applied for our numerical method.

These methods were applied to an instability problem of polar night jets in the stratosphere proposed by Hartmann (1983). The upper bounds were obtained for several profiles of the initial unstable jet and compared with the result of non-linear time integrations by Ishioka and Yoden (1994) and several additional experiments. Revised Shepherd's bound was found to be almost completely identical to our direct bound, which implies that the revised bound gives the tightest bound under the constraints of the conservation of all Casimir invariants and total angular momentum. The revised bound and our direct bound give good estimates of the dependence of the maximum wave-enstrophy obtained in non-linear time integrations on the external parameters which determine the initial jet profiles.

Acknowledgments

The authors thank Peter Haynes and two anonymous reviewers for their very constructive comments on the original manuscript. DMINF1 of the FUJITSU SSL2 Library provided by Data Processing Center, Kyoto University, was used to solve the minimization problem in Section 4, and the GFD-DENNOU Library was used for drawing the figures. K. Ishioka is supported by JSPS Fellowships for Japanese Junior Scientists and this work is supported in part by the Grant-in-Aid for Scientific

Research, the Ministry of Education, Science, and Culture of Japan, and by the Grant-in-Aid for the Cooperative Research with the Center for Climate System Research, University of Tokyo.

Appendix

Derivation of the obvious bound

Using a Legendre expansion, a zonal profile $\overline{q}(\mu)$ can be represented as:

$$\overline{q}(\mu) = \sum_{n=1}^{\infty} a_n P_n(\mu), \tag{34}$$

where $P_n(\mu)$ is a Legendre polynomial defined as:

$$P_n(\mu) \equiv \frac{\sqrt{2n+1}}{2^n n!} \frac{d^n}{d\mu^n}(\mu^2-1)^n, \ (n=1,2,\cdots). \tag{35}$$

In Eq. (34), the summation starts from $n = 1$ not $n = 0$ because $[\overline{q}]$ must be 0 on the spherical domain. The Legendre polynomial $P_n(\mu)$ satisfies the following orthogonal relationship as:

$$\frac{1}{2}\int_{-1}^{1} P_m(\mu)P_n(\mu)d\mu = \delta_{mn}, \tag{36}$$

where δ_{mn} is Kronecker's delta. Then, F_z is represented by a_n as:

$$F_z = \left[\frac{1}{2}\overline{q}^2\right] = \frac{1}{2}\sum_{n=1}^{\infty} a_n^2. \tag{37}$$

Since $P_1(\mu) = \sqrt{3}\mu$, D is represented as:

$$D = [\mu\overline{q}] = \frac{1}{\sqrt{3}}a_1. \tag{38}$$

From Eqs. (37) and (38), F_z takes the minimum value under the conservation of D when $a_1 = \sqrt{3}D$ and $a_n(n \neq 1) = 0$ as:

$$F_z = \frac{1}{2}a_1^2 = \frac{3}{2}D^2. \tag{39}$$

References

Hartmann, D.L., 1983: Barotropic instability of the polar night jet stream. *J. Atmos. Sci.*, **40**, 817–835.

Ishioka, K. and S. Yoden, 1994: Non-linear evolution of a barotropically unstable circumpolar vortex. *J. Meteor. Soc. Japan*, **72**, 63–80.

Luenberger, D.G., 1973: *Introduction to Linear and Nonlinear Programming*, Addison-Wesley, 356pp.

McIntyre, M.E. and T.G. Shepherd, 1987: An exact local conservation theorem for finite-amplitude disturbances to non-parallel shear flows, with remarks on Hamiltonian structure and on Arnol'd's stability theorems. *J. Fluid Mech.*, **181**, 527–565.

Press, W.H., B.P. Flannery, S.A. Teukolsky and W.T. Vetterling, 1992: *Numerical Recipes in FORTRAN: the art of scientific computing — 2nd. ed.*, Cambridge University Press, 963pp.

Shepherd, T.G., 1987: Non-ergodicity of inviscid two-dimensional flow on a beta-plane and on the surface of a rotating sphere. *J. Fluid Mech.*, **184**, 289–302.

Shepherd, T.G., 1988: Rigorous bounds on the nonlinear saturation of instabilities to parallel shear flows. *J. Fluid Mech.*, **196**, 291–322.

順圧不安定による擾乱の発達の上限を求める数値的手法

石岡圭一
（東京大学大学院数理科学研究科）
余田成男
（京都大学大学院理学研究科）

球面上の帯状ジェットの順圧不安定による擾乱の発達に対して、厳密な上限値を求める二種類の数値的手法を提示した。

その一つは、Shepherd (1988)の手法に基づくもので、領域平均された擬運動量密度の保存を利用するものである。ここでは、離散化により、変分最小化問題を準ニュートン法を用いて数値的に解いている。もう一つは、著者らの独自の手法で、すべてのカシミール不変量および全絶対角運 動量の保存則からなる束縛のもとで最小化問題を解くものである。ここでは、2次計画問題を解くために、オペレーションズ・リサーチにおける一手法である凸シンプレックス法を利用している。

これら二種類の手法をいくつかの不安定なジェット分布に適用して上限値を求め、その上限値を、不安定なジェットからの非線形時間発展を高分解能の数値モデルによって計算した結果(Ishioka and Yoden, 1994)と比較した。その結果、得られた二種類の上限値はほとんど完全に等しく、また、これらの上限値は数値実験の結果の1.2から2.3倍の見積りを与えること がわかった。